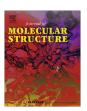
ELSEVIER

Contents lists available at ScienceDirect

Journal of Molecular Structure

journal homepage: www.elsevier.com/locate/molstruc



2D correlation analysis in vibrational sum-frequency generation spectroscopy



Sandra Roy^a, Joshua S. Post^a, Kuo-Kai Hung^b, Ulrike Stege^b, Dennis K. Hore^{a,*}

- ^a Department of Chemistry, University of Victoria, Victoria, British Columbia V8W 3V6, Canada
- ^b Department of Computer Science, University of Victoria, Victoria, British Columbia V8W 3P6, Canada

ARTICLE INFO

Article history:
Available online 9 November 2013

Keywords: Nonlinear optics Vibrational spectroscopy Surface structure Two-dimensional correlation analysis

ABSTRACT

2D correlation analysis provides a powerful means of extracting structural and dynamical data from spectroscopic experiments. This has been successfully developed for techniques such as IR absorption spectroscopy, where the correlation has additionally been shown to increase the spectral resolution by observing the differing behavior of overlapping absorption bands in response to an external perturbation. Visible-infrared sum-frequency generation (SFG) spectroscopy combines many of the benefits of IR absorption and Raman scattering spectroscopy, and adds a unique structural perspective due to its surface specificity. Bringing the flexibility of 2D correlation analysis to SFG experiments would therefore further enhance the power and utility of this nonlinear vibrational spectroscopy. However, straightforward application of the correlation algorithms to homodyne SFG intensity data is not ideal as the SFG line shape often masks underlying spectral features, resulting in misleading correlation maps. We show that application of correlation analysis to heterodyne SFG experiments restores the qualitative utility of such analyses. An example is provided for the case of leucine adsorption onto surfaces of varying hydrophobicity.

© 2013 Elsevier B.V. All rights reserved.

1. Introduction

Vibrational spectroscopy such as IR absorption and Raman scattering have long been regarded for their ability to provide sub-molecular structural details, owing to the localization of vibrational modes, particularly those of high frequency. Together with the high signal-to-noise, spectral resolution, reproducibility, and speed afforded by modern instrumentation, these techniques are unique in their ability to determine fine structural details in solution, solid, and gaseous phases. For the study of chiral molecules, including the characterization of protein secondary and tertiary structure, vibrational circular dichroism (VCD) and Raman optical activity (ROA) are becoming increasingly prevalent [1-7]. As a result of the demonstrated power of these techniques, there is interest in using vibrational spectroscopy to study the surface structure of molecules, whether they are the outermost region of a bulk solid or liquid phase, or are adsorbed species at a solid-liquid, solid-vapour, or liquid-vapour interface. A central challenge associated with the characterization of molecules at interfaces is acquiring sufficient specificity so as to discriminate between nearby molecules in an adjacent bulk phase, as these generally outnumber interfacial species by orders of magnitude. This is where

$$P_i^{(2)} = \sum_{i} \sum_{k} \varepsilon_0 \chi_{ijk}^{(2)} E_j E_k, \tag{1}$$

where ε_0 is the vacuum permittivity. The surface specificity arises from the fact that, under the electric dipole approximation, all elements of $\chi^{(2)}$ vanish in centrosymmetric materials [9,11]. In isotropic phases the only place where the centrosymmetry is broken is at the interface. Of the various second-order nonlinear processes, visible-infrared sum-frequency generation has gained recent attention as a structural probe [12–15]. In this process, a fixed frequency visible laser (with wavelength typically 532 nm from a doubled YAG laser, 800 nm from a Ti:sapphire oscillator, or 1064 nm from the YAG fundamental) and a tunable or broadband IR laser ($\omega_{\rm IR}$ = 1000–4000 cm⁻¹) are annihilated to produce a component of the polarization at the sum-frequency ($\omega_{\rm SFG} = \omega_{\rm vis} + \omega_{\rm IR}$). For example, when using a x-polarized visible laser and a z-polarized IR laser, the contribution to the x component of the nonlinear polarization is given by

$$\varepsilon_0 \chi_{xxz}^{(2)}(-\omega_{SFG}, \omega_{vis}, \omega_{IR}) E_x(\omega_{vis}) E_z(\omega_{IR}).$$
 (2)

second-order nonlinear optical techniques can make a contribution [8–10]. The *i*th component of the second-order polarization is given by the 27-element nonlinear susceptibility tensor $\chi^{(2)}$ and the *i* and *k* components of the applied fields

^{*} Corresponding author. Tel.: +1 2507217168. E-mail address: dkhore@uvic.ca (D.K. Hore).

This oscillating charge distribution in turn re-radiates a field at $\omega_{\rm SFG}$. As the IR laser is tuned over vibrational resonances, an enhancement in $\chi^{(2)}(\omega_{\rm IR})$ is observed that may be linked directly with structural information in a manner analogous to what is done for polarized IR and Raman spectroscopy, but considering the higher-order response function.

It is natural that vibrational SFG spectroscopy should seek to take advantage of techniques that have been established in other forms of vibrational spectroscopy, such as polarization analysis for the quantification of bond orientation distributions [16-19], multidimensional techniques for observing coupling between modes [20,21], isotopic labelling for the selective study of particular moieties [22,23], and two-dimensional correlation analysis (2DCOS) [24-28]. Although generalized 2DCOS is applicable to a broad range of measurements extending beyond spectroscopy, it has been most developed and applied by the vibrational spectroscopy community. The basic idea—to investigate how the spectral response at one frequency ω_1 is correlated to that at another frequency ω_2 in response to an external perturbation—has several advantages. First, it may effectively enhance the spectral resolution in cases where two or more overlapping peaks behave differently. The observation of cross peaks then provides the clue to these band components and their frequencies. Second, it may reveal trends that are not evident in the raw spectra. Third, when the complex cross correlation $X(\omega_1, \omega_2)$ is expressed in terms of synchronous $\Phi(\omega_1,\omega_2)$ and asychronous $\Psi(\omega_1,\omega_2)$ correlation maps

$$X(\omega_1, \omega_2) = \Phi(\omega_1, \omega_2) + i\Psi(\omega_1, \omega_2), \tag{3}$$

Noda's rules [24] may be used to interpret the cross peaks in order to arrive at the causality relationship between events. Finally, the intensity of autopeaks in the synchronous map are a direct measure of the degree to which a particular feature in the spectrum is changing, irrespective of the extent to which that component is represented in the overall spectrum. These appealing aspects of 2DCOS applied to vibrational spectroscopy have found recent applications in the discrimination of water solvation environments [29,30], polymer dynamics [31–33] protein structure determination [34–39], the quality control of pharmaceuticals [40,41], and in the study of the 2DCOS signatures of cells [42,43].

It would be appealing to extend the toolbox of techniques that have been applied to vibrational SFG to include 2DCOS. The resolution enhancement in particular would be most welcome, as most current SFG experiments are typically ≈5 cm⁻¹ resolution for scanning instruments (picosecond pulses) and $\approx 10-15$ cm⁻¹ for broadband instruments (femtosecond pulses). Although recent developments increase the spectral resolution [44,45], a fundamental obstacle has to do with the SFG lineshape as obtained in a homodyne experiment that measures $|\chi^{(2)}|^2(\omega_{\rm IR})$. On account of the fact that the contribution from participating vibrational modes are summed before the response is squared, interferences may lead to odd features in the raw spectra, particularly in cases where the peaks are overlapping or the spectral resolution is not sufficiently high. In the following section we will demonstrate that, compared to an IR absorption experiment, 2DCOS applied to homodyne SFG has advantages and disadvantages. We then consider a heterodyne experiment where the SFG field generated by the sample is interfered with a reference SFG (local oscillator) field, to provide information on the complex-valued $\chi^{(2)}(\omega_{\rm IR})$ that may then be expressed as its imaginary component [46-58]. We will show that 2DCOS applied to $\text{Im}[\chi^{(2)}(\omega_{\text{IR}})]$ has clear advantages and overcomes all of the obstacles encountered in $|\chi^{(2)}|^2$ correlation analysis. In the final section, we will provide a demonstration of the application of 2DCOS-SFG spectroscopy to the study of leucine adsorption onto surfaces of varying hydrophobicity. Here we will consider the hydrophobicity of a model surface to be the external perturbation, and study the adsorbed leucine polarized IR

absorption and $\text{Im}[\chi^{(2)}(\omega_{\text{IR}})]$ response as generated from molecular dynamics simulations through 2DCOS analysis.

2. Application of correlation analysis to vibrational sum-frequency generation spectra

2.1. Spectral line shapes

To illustrate the application of 2D correlation analysis, we have generated dynamic spectra for an IR absorption lineshape

$$I_{\rm Abs}(\omega_{\rm IR},t) \propto \sum_{j=1}^{7} \frac{A_j^2(t)\Gamma_j}{\left(\omega_j - \omega_{\rm IR}\right)^2 + \Gamma_j^2}, \tag{4}$$

where $A_j(t)$ is the time-dependent amplitude, ω_j is the frequency, and Γ_j is the width of each resonant mode. Here we are considering a time evolution of the spectral shape in response to an arbitrary perturbation with $A_j(t) = \sin a_j(t)$, where a range of a_j were generated such that $A_j(t)$ varies from A_0 at t=0 to A' at t=t' according to the values of these parameters as given in Table 1. For the SFG spectra, we concern ourselves with the second-order nonlinear susceptibility

$$\chi^{(2)}(\omega_{\rm IR},t) = \sum_{j=1}^{7} \frac{A_j(t)}{\omega_j - \omega_{\rm IR} - i\Gamma_j}.$$
 (5)

A trigonometric function was used for the amplitude since, as will be discussed further below, we wish to consider positive and negative values of A(t). In a homodyne SFG experiment, the measured intensity is proportional to the squared magnitude of the second order susceptibility $|\chi^{(2)}|^2$

$$|\chi^{(2)}|^2(\omega_{\mathrm{IR}},t) = \left| \sum_{i=1}^7 \frac{A_j(t)}{\omega_j - \omega_{\mathrm{IR}} - i\Gamma_j} \right|^2. \tag{6}$$

In a heterodyne SFG experiment, one has access to the imaginary component of $\chi^{(2)}$. These spectra have a simpler lineshape

$$\operatorname{Im}[\chi^{(2)}(\omega_{\mathrm{IR}},t)] = \sum_{j=1}^{7} \frac{A_{j}(t)\Gamma_{j}}{(\omega_{j} - \omega_{\mathrm{IR}}) + \Gamma_{j}^{2}},\tag{7}$$

as the dispersive component has been removed. Seven resonances were selected in order to best illustrate the differences between these two experimental lineshapes. In order to additionally compare these three different spectroscopic techniques in terms of their effect on the asynchronous component of the correlation, we have delayed the time evolution of some spectral features with respect to others. This delay is shown in the last column of Table 1 in terms of the fraction of the time period. For example, a delay of 0.25 for the feature at 2880 cm⁻¹ indicates that the evolution of this band does not start until a quarter of the measurement time has elapsed in comparison to a band with no delay, such as the one at 2820 cm⁻¹. As an example, we illustrate the evolution of the peak

Table 1 Parameters used to model the 7 peaks for the IR absorption, $|\chi^{(2)}|^2$, and $\text{Im}[\chi^{(2)}]$ spectra. The initial amplitude A_0 and final amplitude A' is listed, along with the fraction of total time that the amplitude remains at A_0 before it increases or decreases towards A'

ω/cm^{-1}	$A_0/a.u.$	A'/a.u.	Delay/period
2820	0.34	0.71	0.00
2840	0.00	-0.50	0.50
2860	-0.64	0.53	0.10
2880	0.34	-0.64	0.25
2900	-0.87	-0.34	0.00
2920	0.00	0.50	0.00
2940	0.87	0.34	0.00

Download English Version:

https://daneshyari.com/en/article/1402480

Download Persian Version:

https://daneshyari.com/article/1402480

<u>Daneshyari.com</u>